Facile synthesis of a Ag/AgCl/BiOCl composite photocatalyst for visible – light – driven pollutant removal

Dorcas O. Adenuga*, Shepherd M. Tichapondwa and Evans M.N. Chirwa

Water Utilization Division, Chemical Engineering Department, University of Pretoria, South Africa

*Corresponding author. Water Utilization Division, Chemical Engineering Department, University of Pretoria, South Africa

Highlights

• Facile synthesis of ternary Ag/AgCl/BiOCl photocatalyst.
• In-depth characterization through various methods of synthesized material samples.
• Reduced bandgap as a result of SPR heterojunction coupling.
• Enhanced photocatalytic activity in visible light degradation of phenol.

Abstract

Forerunner investigators of photocatalysis utilized TiO_2 as the photocatalyst of choice. It has major drawbacks of which the most important one is that it is only activated under ultraviolet (UV) light irradiation. This high energy consumption made the process practically unfeasible. Solar energy (natural light and heat from sun) has great prospects with regards to acting as a substitute for UV light since it is a renewable and cheaper energy source. In this work, the development of a heterogeneous silver/ silver chloride/ bismuth oxychloride (Ag/AgCl/BiOCl) photocatalyst that is able to utilize natural light through visible light activation was investigated. This will successfully serve as a green alternative in the use of renewable energy for pollution reduction while saving energy. The synthesized photocatalysts were characterized using various techniques. The purity and crystallinity of the synthesized photocatalysts were determined using x-ray diffraction (XRD) while x-ray photoelectron spectroscopy (XPS) was used to determine the elemental composition and chemical states present in the synthesized catalysts as well as confirm the presence of elemental Ag. Fourier-transform infrared spectroscopy (FTIR) specified the functional groups present while the morphology and chemical composition were determined using a scanning electron microscopy (SEM) coupled with energy dispersive X-ray spectroscopy (EDS) and transmission electron microscopy (TEM). The surface area and pore size were measured on a Brunauer-Emmett-Teller (BET) and thermogravimetric analysis (TGA) was done to determine the thermal degradation of synthesized particles. Ultraviolet-visible spectroscopy (UV–vis) was done to determine the photoabsorption range and bandgap of the particles as efficiency of photocatalysis is dependent on these properties together with the morphology of the semiconductor material. Ag/AgCl/BiOCl photocatalyst showed good photocatalytic activity of 52 % under a low-wattage simulated visible light irradiation in 4 h. This work therefore shows great prospect for pollution control through energy reduction thereby protecting the environment.

Keywords: BiOCl; Ag/AgCl; Degradation; Phenol; Photocatalysis; Visible light

1. Introduction

Semiconductor photocatalysis, a version of advanced oxidation process (AOP), has shown potential for treatment of contaminants in water especially where the water is contaminated with micro pollutants and complex organic materials [1]. Due to its ability to completely mineralize organic pollutants leaving no traces of the compound, photocatalysis has been referred to as a "Clean" technology. Potentially, photocatalysis can also be classified as a "Green or fossil energy free" technology if solar radiation is used with the catalysts. Photocatalysis has been tested in the destruction of bacteria and virus, cancer cells inactivation, odour mitigation, water photo splitting and oil spillage clean-ups [2]. Photocatalysis involves the use of a semiconductor catalysts suspended in aqueous medium which when illuminated results in the production of photogenerated holes and electrons on the surface of the catalyst. This enables toxic pollutants to be degraded into non-toxic and non-hazardous compounds such as water, carbon dioxide and other small molecules [3]. Titanium based photocatalysts have been widely used due to their relatively low cost, stability and inertness in aquatic systems [4]. However, titanium based photocatalysts are characterized by their high electron-hole recombination rates, low quantum yields and wide band-gap energy which makes them unsuitable for visible light activation and only viable for activation and usage in the ultraviolet light region [5].

Other semiconductor catalysts grouped as oxides, sulphides, oxysulfides, nitrides and oxynitrides have gained attention due to their potential application for solar energy conversion and their ability to degrade environmental pollutants [6]. This is advantageous because visible light represents 45 % of the solar spectrum and a visible light activated catalyst will enable the use of solar energy for photocatalysis [7,8].

While various strategies have been explored to improve the bandgap of available photocatalysts such as TiO_2 into the visible light range, researchers in water remediation have introduced doping, metal loading and heterojunctions by matching band potentials to extend semiconductors into the visible light range [9,10]. These photocatalysts are specially designed to ensure higher photocatalytic activity because of adequate separation of electron-hole pairs thereby improving their visible light activation response [11]. Several heterojunction mechanisms have proven to be successful in improving the activity of photocatalysts, these includes type-II and p-n heterojunctions. While p-n heterojunctions have proved to be more superior, new heterojunction methods namely surface and direct Z-scheme heterojunctions have recently received considerable attention [10].

Examples of catalysts being investigated in recent years include bismuth-based oxyhalides. This is due to their uncommon properties of layered structures and their demonstrated potential for activation in a wide electromagnetic band including the visible light range. The bismuth-based oxyhalides have been tested in catalysis, nanodevice and nanosensor development and in eco-friendly pigments [6,12]. The layered structure of bismuth oxyhalides provides a large enough space for the atoms and orbitals to be polarised thereby separating the electron-hole pair effectively and reducing recombination of the generated electron-hole pairs. Bismuth oxychloride (BiOCl) is one of the bismuth oxyhalides which has attracted vast attention due to its high photocatalytic activity evidenced in the degradation of cationic dyes such as methylene blue and rhodamine blue [13].

Table 1. Photocatalytic degradation of different Ag/AgCl-composite particles in previous studies.

Photocatalyst	Pollutant	Investigation	Remarks	Reference
Hollow Ag/AgCl/BiOCl	Methyl orange (MO)	Ag/AgCl/BiOCl synthesis, characterization and photodegradation of MO using a 5 W LED visible light.	20 % Ag/AgCl/BiOCl showed high photocatalytic activity for MO under LED irradiation. h^+ and $\cdot O^-$ plays significant role in MO degradation.	[5]
Flower-like Ag/AgCl/BiOCl	RhodamineB, Tetracycline	Synthesis through a solvothermal method, characterization, visible light degradation of pollutants using a 500 W Xe lamp. Recycling of catalysts.	Followed first order kinetics. Ag/AgCl/BiOCl shows a higher photocatalytic activity in visible light than pure BiOCl.	[19]
Ag/AgCl/BiOCl nanosheets	*S. aureus*	Synthesis, characterization, photocatalytic inactivation of bacteria using a 500 W Xe lamp, inactivation mechanism proposed.	Ag/AgCl/BiOCl showed higher photocatalytic activity in comparison to Ag/BiOCl, AgCl/BiOCl and Ag/AgCl/TiO_2.	[20]
AgCl nanotubes/BiOCl nanosheets	Methyl orange	Synthesis, characterization, degradation, catalyst recyle and nanosheet/nanotubes degradation mechanism.	Followed pseudo-first order kinetics. Strong visible light response and improved separation of photogenerated electron holes.	[21]
Ag/AgCl/WO_3-nanoflakes	4-Aminobenzoic acid (4-ABA)	Synthesis in geothermal water (chlorine source), visible light degradation of pollutant using a 300 W xenon lamp, stability test and degradation mechanism.	The 50 wt % Ag/AgCl/WO_3 showed a higher photocatalytic activity under visible light irradiation in comparison to Ag/AgCl and WO_3.	[22]
Poly(N-hexadecyl pyridine acetylenic alchohols bromide)-Ag/AgCl (Pp-16@Ag/AgCl)	Rhodamine B and fast green dyes	Synthesis, characterization of photocatalyst, its degradation of pollutants and reusability tests.	The composite showed high photocatalyst activity in the degradation of RB and FG under UV irradiation.	[23]
Ag/AgCl dispersed on mesoporous Al_2O_3	Methylene orange and methylene blue	Synthesis, characterization, and degradation of pollutants under a 300 W Xe arch lamp for visible light irradiation.	The photocatalysts exhibited high photocatalytic activity and stability in the degradation of the organic pollutants. Ag/AgCl(Ch_3COOAg)/Al_2O_3 showed the highest photocatalytic activity.	[24]
Ag/AgCl/SnO_2	Rhodamine B	Synthesis, characaterization, degradation of pollutants under simulated sunlight irradiation with a 500 W xe lamp used as light source.	Successful synthesis of Ag/AgCl/SnO_2 and its different Ag/Sn molar ratios. Ag/Sn shows that 7% shows the the best photocatalytic activity.	[25]
Ag/AgCl/WO_3	Rhodamine B	Microwave assisted synthesis of Ag/AgCl/WO_3, photocatalyst characterization and its photocatalytic activity under simulated solar light.	The photocatalyst activity of the synthesized photocatalyst in the degradation of dye is noticed to be higher in than WO_3.	[26]

Photocatalyst	Pollutant	Investigation	Remarks	Reference
Cyclized polyacrylonitrile (CPAN)/Ag/AgCl	Methyl orange, rhodamine blue	Synthesis, characterization and photocatalytic activity test of photocatalyst in the degradation of organic pollutants under visible light irradiation using a 300 W iodine tungsten lamp as a lamp source.	The synthesized catalyst showed great activity and stability in the degradation of methyl orange.	[27]
Ag/AgCl-$CdWO_4$	Rhodamine blue, Methylene blue, methylene orange, phenol	Catalyst synthesis through photoreduction process, characterization and degradation under visible light with a 300 W xenon lamp as light source.	Complete degradation of RhB, MB and MO using synthesized catalyst in 30 min. 95 % Phenol degradation in 90 min.	[28]
Cu_2O/Ag/AgCl microcubes	Methyl orange	Synthesis, characterization and visible light activated degradation of MO using a 500 W Xe lamp.	93 % methyl orange degradation in 16 min. High stability of synthesized catalyst.	[29]
TiO_2 hollow nanofibers grafted Ag/AgCl (Ag/AgCl-ElTiO_2)	Methyl orange	Synthesis through electrospinning and co-precipitation, characterization and degradation of MO under visible light (300 W Xe arc lamp) degradation.	Ag/AgCl-ELTiO_2 showed a higher photocatalytic activity in comparison to Ag/AgCl-SGTiO_2, Ag/AgCl, ELTiO_2 and SGTiO_2.	[30]
AgCl@Sn-TiO_2 microspheres	Rhodamine blue, 3-aminophenol	Simple hydrothermal synthesis, characterization and photodegradation of contaminants under visible light.	The synthesized catalyst showed great photocatalytic activity in the degradation of the pollutants and it is noted that the photocatalytic activity is based on the amount of AgCl present in the composite.	[31]
Ag-AgCL in porous PVA	Methyl orange	Three–step synthesis, characterization, visible light degradation under visible light (xenon lamp) and photostability tests.	Ag/AgX has a photoactivity dependence on Cl. The synthesized AgCl/PVA showed week photoactivity under acidic conditions.	[12]
AgCl/Ag-cellulose paper	*E. coli, S. aureus, S. epidermidis, P. aeruginosa*, Methyl blue	Synthesis through a facile ultra-sound agitation process, degradation of organic pollutant under direct sunlight, antibacterial and biocompatibility tests.	Successful fabrication of AgCl/Ag hybride cellulose paper as confirmed by characterisation. Synthesized catalyst showed superior photoactivity in the inactivation of bacteria and degradation of organic pollutant.	[32]
Ag/AgCl@TiO_2	4-chlorophenol, Cr(VI)	Synthesis through a deposition, precipitation and reduction method. Characterization of synthesized catalyst and degradation of 4-chlorophenol and photoreduction of Cr(VI) under visible light irradiation.	Successful one-pot synthesis of photocatalyst. Efficient photodegradation of 4-CB and Cr(VI) under visible light. Ag to AgCl ratio discovered to be key component in photoactivity.	[33]

Different synthesis techniques are used to produce BiOCl. Depending on the process used, different crystalline structures and macroparticles are produced, such as, nanoflowers, nanorods, nanosheets, nanobelts, thin films which all have different morphology and surface area, consequently affecting the band gaps and photodegradation potential [14,15]. BiOCl, like TiO_2, exhibits a wide band gap and therefore, is mainly activated within the UV range [16]. This has led to research into improving the visible light responsiveness of BiOCl. Some good materials were discovered for this purpose, one of which is the AgX (X = Cl, Br, I). AgX has a wide band-gap and therefore cannot be photo-excited under visible light irradiation [17], however, its ability to photoreduce upon light illumination and form elemental Ag with surface plasmon resonance (SPR) properties has been shown to drastically improve the visible light responsiveness of some large band-gap semiconductors [18]. Previous work has shown that Ag/AgX/BiOX possesses good photodegradation activity in the degradation of dyes and organism sterilization [5]. Table 1 summarizes the various Ag/AgCl/-catalyst photocatalytic heterojunction systems that have been used to degrade different organic contaminants in previous studies.

In the present work, we report the synthesis of Ag/AgCl/BiOCl composite photocatalysts fabricated through the deposition of AgCl on BiOCl followed by the introduction of elemental Ag on the surface through photoreduction. The constituent components, AgCl and BiOCl were also synthesized. The material properties of these particles were characterised using a range of analytical techniques. The photocatalytic activity of all synthesized materials was investigated by monitoring the degradation of phenol under both UV and visible light and a possible photocatalytic mechanism was suggested. Our investigation contributes to the body of knowledge around Ag/AgCl based photocatalysts used in the degradation of organic contaminants in waste water under visible light. To the best of our knowledge, the visible light driven photoactivity of the present ternary catalyst and its individual constituents on phenol contaminated wastewater has not yet been reported.

2. Materials and methods

2.1. Photocatalyst synthesis

Table 2 summarizes the main materials that were used to synthesize the various catalysts presented in this study.

Table 2.: Materials used for catalyst synthesis and their source.

Material	Source
Cetyltrimethylammonium chloride (CTAC)	Sigma-Aldrich
Bismuth (III) nitrate pentahydrate ($Bi(NO_3)_3.5H_2O$)	Sigma-Aldrich
Phenol	Merck, SA
Acetic acid	Glassworld, SA
Silver nitrate ($AgNO_3$)	Glassworld, SA

The synthesis method used to prepare Ag/AgCl/BiOCl composite photocatalyst was adapted from Hong et al. [34]. Bismuth oxychloride particles were synthesized by dissolving 9.7 g of $Bi(NO_3)_3.5H_2O$ into a solution containing 30 mL ultrapure water and 15 mL acetic acid. A second solution was prepared by dissolving 6.4 g of cetyltrimethylammonium chloride (CTAC) in 30 mL of ultrapure water. The bismuth nitrate solution was then added dropwise into the CTAC solution with constant stirring at room temperature for an hour. A white

precipitate was formed and recovered by filtration. It was then washed three times with ethanol and three times with ultrapure water before being dried overnight at 70 °C. The resultant particles were ground to fine powder.

AgCl was synthesized through an in situ precipitation method. 3.2 g of CTAC was added to 30 mL of ultrapure water in one beaker. In another beaker, 3.4 g of $AgNO_3$ was added to 70 mL of ultrapure water. Both solutions were mixed and stirred in the dark for five hours followed by washing three times with ethanol and water before being dried at 80 °C for 8 h.

2.1.1. Synthesis of Silver chloride/bismuth oxychloride (AgCl/BiOCl) and silver/silver chloride/bismuth oxychloride (Ag/AgCl/BiOCl)

Finally, the composite silver chloride/bismuth oxychloride (AgCl/BiOCl) and silver/silver chloride/bismuth oxychloride (Ag/AgCl/BiOCl) catalysts were synthesized as follows. 1.7 g of silver nitrate ($AgNO_3$) was dissolved in 925 mL of ultrapure water. Ag/AgCl/BiOCl composites was synthesized by mixing the silver nitrate solution with a BiOCl solution similar to the one described for the BiOCl synthesis. The solution was magnetically stirred for 6 h. The resultant precipitate was collected and re-dispersed in 1 L of water before irradiating it with a 36 W visible light lamp for 1 h for the photoreduction of Ag^0. AgCl/BiOCl composite catalyst synthesis followed a similar synthesis route with the exception of the photoreduction step.

2.2. Characterization techniques

The crystalline purity and phases present in the synthesized particles were evaluated using X-ray diffraction (XRD). The spectra were recorded on a PANalytical X'Pert Pro powder diffractometer in θ–θ configuration with an X'Celerator detector, variable divergence- and fixed receiving slits with Fe filtered Co-Kα radiation (λ = 1.789 Å). The primary functional groups on the catalyst surfaces were determined using a Perkin Elmer Fourier-transform infrared (FTIR) spectrometer with a MIRacle Zn/Se ATR attachment. The Brunauer-Emmett-Teller (BET) surface area and porosity of the particles was obtained using a Micromeritics TriStar II analyser. The primary particle size, morphology and EDS mapping of the synthesized photocatalysts were captured on a scanning electron microscopy (SEM) Zeiss Ultra PLUS FEG SEM. SEM samples were prepared by distributing the particles on an aluminum plate and coated with carbon using an auto-coating sputter coater. SEM images were captured at 1 kV. TEM images were captured using a JEOL JEM 2100 F TEM. The samples were placed on a TEM mesh grid and coated with a light layer of carbon for stabilization. The valence states of the elements contained in the photocatalysts were confirmed through X-ray photon spectroscopy (XPS) on a Thermo ESCALAB 250Xi and using a monochromatic Al Kα X-ray source (1486.7 eV) operated at 300 W. This was accomplished by measuring the kinetic energy of electrons deflected from the surface of the catalyst. The thermal stability of the synthesized particles was determined using a TGA5500 from TA instruments. The analysis was carried out in a temperature range of 25–1000 ºC, at a heating rate of 10 ºC min^{-1} in an inert nitrogen atmosphere. The photoelectric properties of the photocatalyst material was evaluated by recording the UV–vis spectra on a Hitachi U-3900 spectrophotometer.

2.3. Photocatalytic activity evaluation

The photocatalytic activity of the synthesized photocatalysts, was investigated for phenol degradation under both UV and simulated solar light. A batch reactor set-up was used and this consisted of a 400 mL beaker loaded with 300 mL of 10 ppm phenol solution with varying catalyst loading in the range of 0–1 g of catalyst [35]. The experimental sequence involved continuous stirring for 30 min in the dark in order to attain adsorption-desorption equilibrium followed by 4 h of light irradiation. A Philips 36 W UV lamp was used as UV light source while a combination of six, 36 W Fluora lamps normally used for algae growth were used as a visible light source. During the photocatalytic degradation process, 2 mL samples were withdrawn at 30 min intervals, centrifuged and filtered through 0.45 μm membrane filters to remove particles before analysis. Phenol concentration before and after degradation were monitored on a Waters high pressure liquid chromatograph with a photodiode array – Waters 2998 PDA detector using a Waters PAH C18 (4.6 × 250 mm, 5 μm) column. Mobile phase consisted of two solvents A and B where A consists of 1% acetic acid in water and B consists of 1% acetic acid in acetonitrile with phenol elution done at 30 % A and 70 % B.

3. Results and discussion

3.1. Characterization

3.1.1. XRD, FTIR and BET analysis

The purity and crystallinity of the synthesized particles were investigated by XRD analysis. Fig. 1 shows the spectra obtained for the BiOCl, AgCl/BiOCl and Ag/AgCl/BiOCl catalysts. Based on the ICSD database using the X'Pert Highscore plus software, pristine peaks of the pure compounds were detected with virtually no other diffraction peaks being shown. These results indicate that the synthesis procedure was successful and highly crystalline and pure compounds were prepared. Fig. 1 also revealed that near symmetrical spectra were obtained for both the AgCl/BiOCl and Ag/AgCl/BiOCl catalysts. It is worth noting that no elemental Ag was detected in the ternary Ag/AgCl/BiOCl composite photocatalyst. The beam used for X-ray diffraction is known to have an average sample penetration depth of ≈ 2–3 μm [36]. This is larger than the typical size of silver nanoparticles (2 nm – 100 nm) [37] that were expected to form on the catalyst surface. Therefore, it is possible that the Ag° were XRD invisible especially at the very low Ag° concentrations expected. Additionally, the Ag° could have been amorphous making it difficult to detect using XRD analysis. The peaks indexed at $2\theta = 32.2^{\circ}$ and 55.2° were attributed to AgCl and correspond to the (200) and (222) khl planes [11,38]. This observation confirms the coexistence of the AgCl and BiOCl phases.

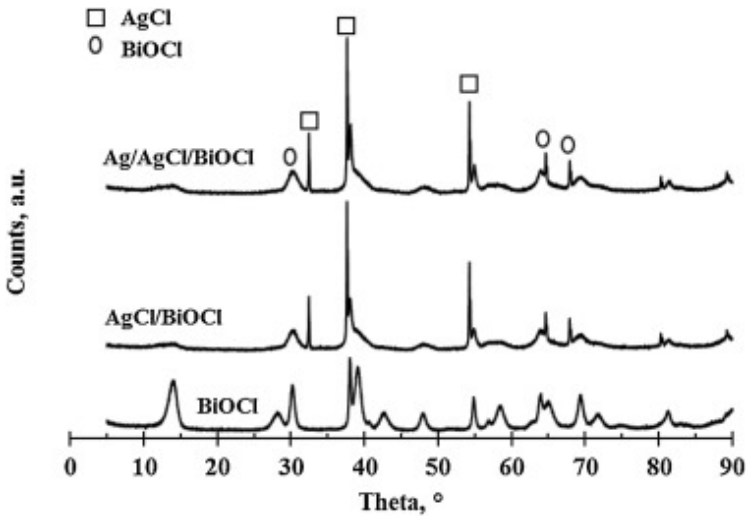

Fig. 1. XRD patterns of BiOCl, AgCl/BiOCl and Ag/AgCl/BiOCl.

FTIR spectroscopy was conducted in order to determine the major functional groups present on the synthesized catalysts. Fig. 2 presents the spectra obtained in the wave number range 550 to 4000 cm^{-1}. The broad band ranging from 3400 – 3500 cm^{-1} was attributed to the O—H group which is a result of the interactions with water. Vibration bands at 2923 cm^{-1} and 1357 cm^{-1} were assigned to the carboxyl and alkane functional groups. This was a surprising result since the synthesized compounds are supposed to be inorganic in nature. The presence of these functional groups was thought to result from remnants of the synthesis process such as CTAC and acetic acid [39] due to inadequate washing. The band at 550 cm^{-1} is attributed to the Bi-O functional group [40] which is a characteristic and present in BiOCl, AgCl/BiOCl and Ag/AgCl/BiOCl.

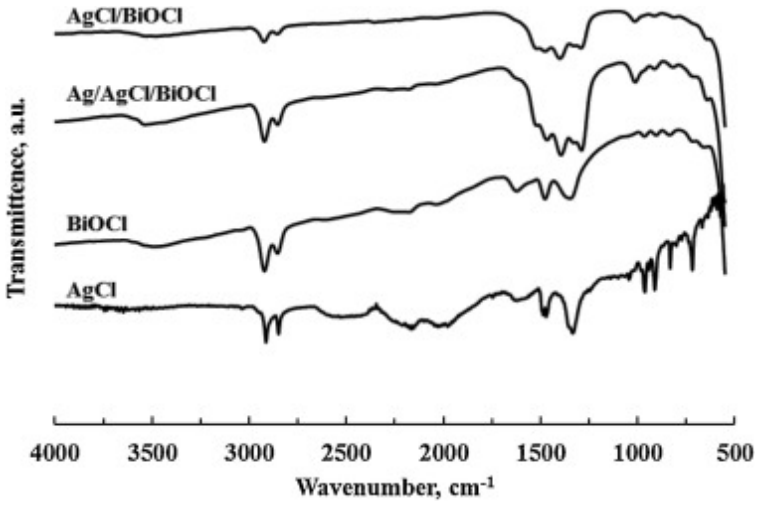

Fig. 2. FTIR spectra for AgCl, BiOCl, AgCl/BiOCl and Ag/AgCl/BiOCl.

The multipoint BET surface area of the ternary Ag/AgCl/BiOCl composite catalyst was 6.64 m^2/g whilst the AgCl and BiOCl recorded values of 8.43 and 4.7 m^2/g, respectively. The pore size (7.0457 nm) and pore volume (0.0187 m^3/g) of the main Ag/AgCl/BiOCl catalyst were also determined.

3.1.2. Particle morphology

The morphology of the various catalysts was evaluated using scanning electron microscopy. The resulting micrograms for the different constituents are shown in Fig. 3(a–d). AgCl particles (Fig. 3a) consisted of an agglomeration of near-spherical particles with the primary particle size ranging from ≈ 200 nm to 1 μm. The BiOCl particles shown in Fig. 3b consist of rod-like structures assembled to form spheres and sheets. A spherical, flower-like morphology was obtained for both the AgCl/BiOCl (Fig. 3c) and Ag/AgCl/BiOCl (Fig. 3d). The TEM image for the ternary Ag/AgCl/BiOCl (Fig. 3e) shows the spherical Ag/AgCl assembled on BiOCl. This flower-like morphology has a potential to improve the photocatalytic properties of the synthesized materials. The layered structure provides enough space for polarisation of atoms and orbitals thereby effectively separating the photogenerated holes and electrons which enhance their photocatalytic activity [41].

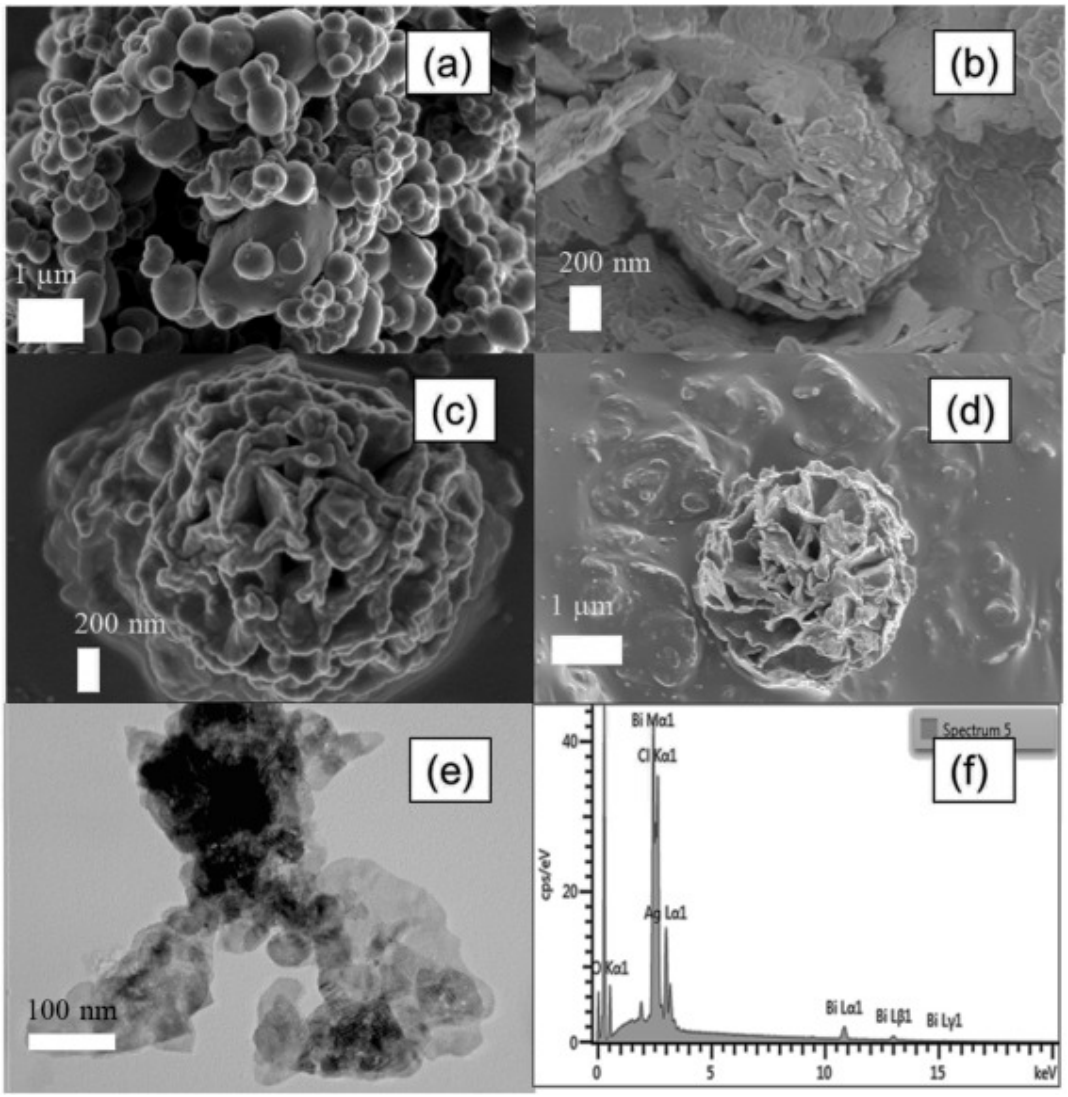

Fig. 3. SEM images of (a) AgCl, (b) BiOCl, (c) AgCl/BiOCl, (d) Ag/AgCl/BiOCl, (e) TEM image of Ag/AgCl/BiOCl, (f) EDS spectra of Ag/AgCl/BiOCl.

SEM-EDS analysis was further carried out to determine the elemental composition. The corresponding spectrum (Fig. 3f), distribution of elements (Table 3) and elemental mapping (SI Fig. 1) on the surface of the synthesized ternary photocatalyst shows the co-existence of Ag, Bi, Cl, and O elements in the synthesized particles. AgCl shows an approximate 1:1 ratio of Ag to Cl in the synthesized AgCl photocatalyst. In BiOCl, AgCl/BiOCl and Ag/AgCl/BiOCl, while oxygen is in excess, the at.% of Ag:Bi:Cl is at an approximate 1:1:2 ratio. The BiOCl, AgCl/BiOCl and Ag/AgCl/BiOCl all show a consistent amount of oxygen present in the synthesized materials which is also similar to work done by Zhao et al. (2018).

Table 3. SEM-EDS atomic percentage of elements in the synthesized photocatalysts.

Elements/ at.%	AgCl	BiOCl	AgCl/BiOCl	Ag/AgCl/BiOCl
Ag	51.54	–	10.92	9.99
Cl	48.46	19.42	22.79	20.28
Bi	–	17.72	12.29	10.55
O	–	62.86	54.01	59.18

3.1.3. XPS analysis

XPS measurements were carried out in order to determine the elemental compositions and specify the chemical states of elements present in the synthesized catalysts. Fig. 4 shows the full XPS spectra for AgCl, BiOCl, AgCl/BiOCl and Ag/AgCl/BiOCl, while Fig. 5 shows the peaks of the different elements present. The two strong peaks at 158.3 eV and 164 eV in the ternary Ag/AgCl/BiOCl, binary AgCl/BiOCl composite and BiOCl can be ascribed to the Bi $4f_{7/2}$ and Bi $4f_{5/2}$ of Bi^{3+} which represents the Bi^{3+} species in BiOCl. The peak at 367.1 eV in AgCl, AgCl/BiOCl and Ag/AgCl/BiOCl corresponds to Ag $3d_{5/2}$. Cui et al. [42] suggests that the peaks at 367.1 eV is attributed to oxidized Ag^{+} in the AgCl while the peak in close proximity at 374 eV is assigned to metallic Ag which is as a result of photoreduction of Ag^{+} to Ag°. It is worth noting that this observation supports presence of Ag° after light irradiation which had previously not been confirmed by the XRD results. The peak at 530.4 eV corresponds to O 1s which is the Bi-O in BiOCl and peak at 197.8 eV corresponds to Cl $2p_{3/2}$. The carbon peak present at 284.9 eV is C 1s which is ascribed to the presence of accidental/adventitious carbon species.

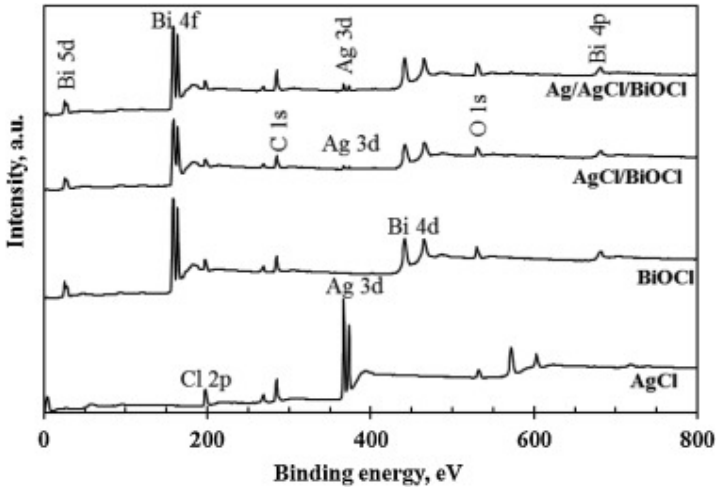

Fig. 4. XPS analysis of synthesized AgCl, BiOCl, AgCl/BiOCl and Ag/AgCl/BiOCl sample.

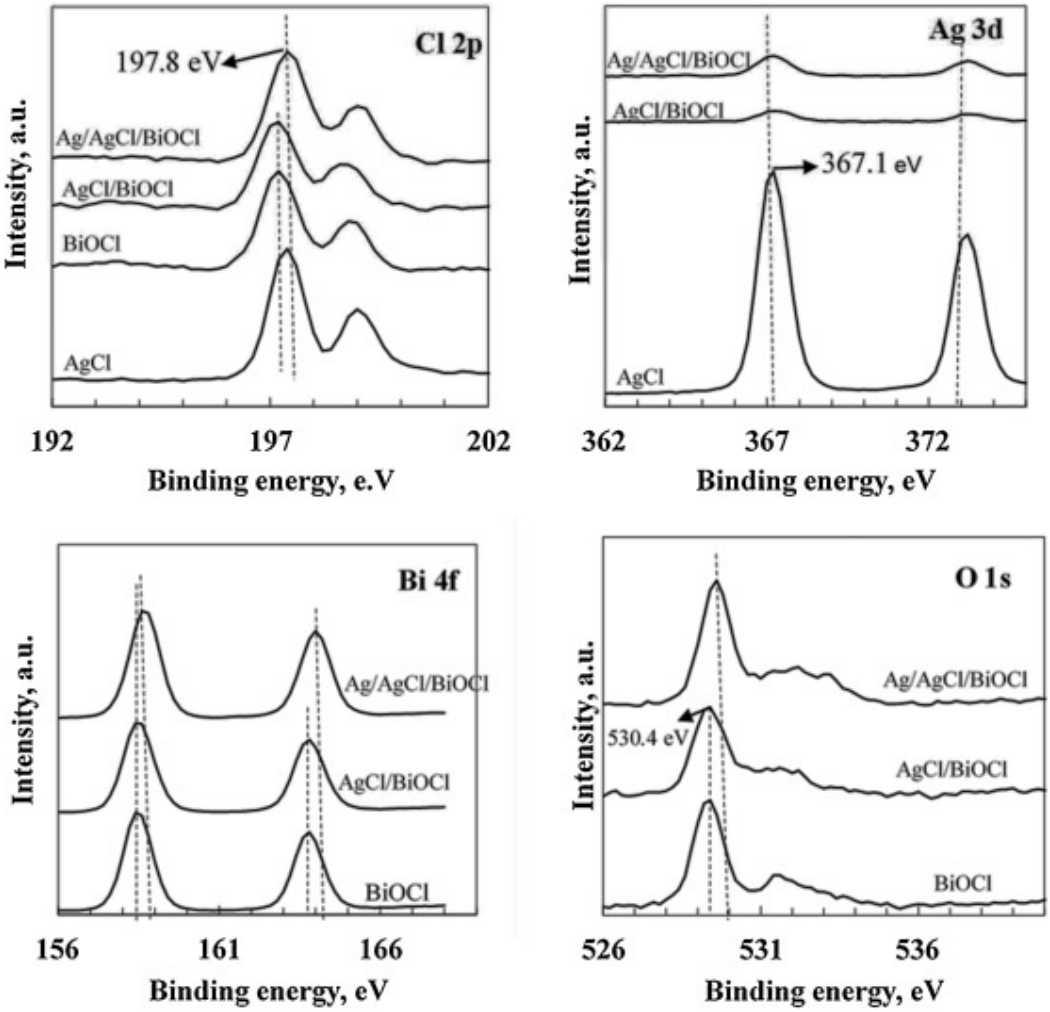

Fig. 5. Corresponding XPS spectra for Cl2p, Ag3d, Bi4f and O1 s in AgCl, BiOCl, AgCl/BiOCl and Ag/AgCl/BiOCl samples.

3.1.4. TGA analysis

The thermal stability of the synthesized photocatalysts was analyzed using TG analysis and the resulting mass loss vs temperature curves are shown in SI Fig. 2. The thermal degradation of the AgCl/BiOCl and Ag/AgCl/BiOCl are identical as the curves are superimposed on each other. At 1000 ºC, AgCl is completely decomposed and BiOCl had an 80 % mass loss while the binary and ternary composites measured a 62 % loss. This shows that AgCl and BiOCl decomposes at a lower temperature in comparison to the synthesized AgCl/BiOCl and Ag/AgCl/BiOCl composites.

3.1.5. UV–vis and band gap measurement

The photoelectric properties of the synthesized catalysts were determined using UV–vis spectroscopy, the resulting spectra are shown in Fig. 6. All the catalysts exhibited absorption in the UV range. More importantly, AgCl/BiOCl showed heightened photoabsorption in the visible light range compared to the other photocatalysts. This was closely followed by Ag/AgCl/BiOCl and BiOCl with AgCl showing virtually no photoabsorption in the visible

light range. These observations suggest that the coupling of AgCl with BiOCl does indeed improve the photoabsorption of the composite in the visible light range. The optical band-gaps were calculated using the Kubelka-Munk equation [43]. The estimated band gaps for the synthesized catalysts were 5.6 eV for AgCl, 5.4 eV for BiOCl, 3 eV for AgCl/BiOCl and 2.8 eV for Ag/AgCl/BiOCl as shown in Fig. 7. These values were higher compared to those reported in literature. Chen et al. [44] measured a band energy of 3.29 eV for BiOCl and 2.9 eV for their hollow structured 30 % Ag/AgCl/BiOCl microspheres. Although, the present study measures a relatively higher bandgap for AgCl and BiOCl, it also shows a significant reduction in bandgap when both materials are coupled.

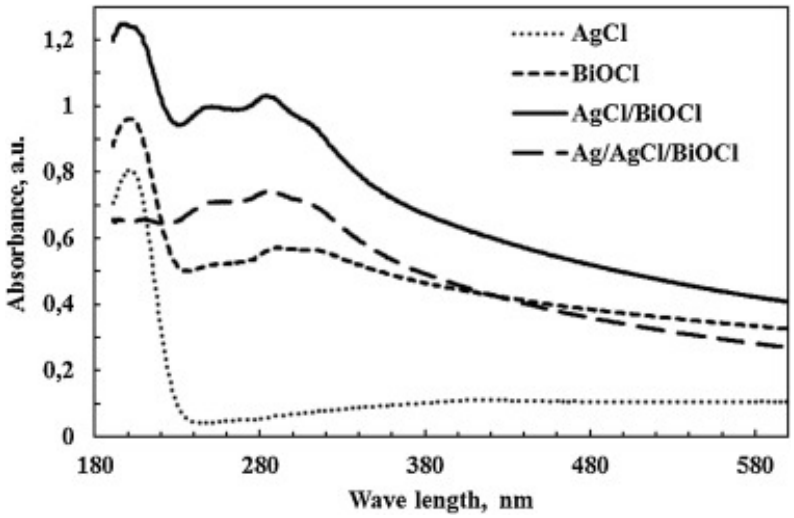

Fig. 6. UV–vis spectra of synthesized particles.

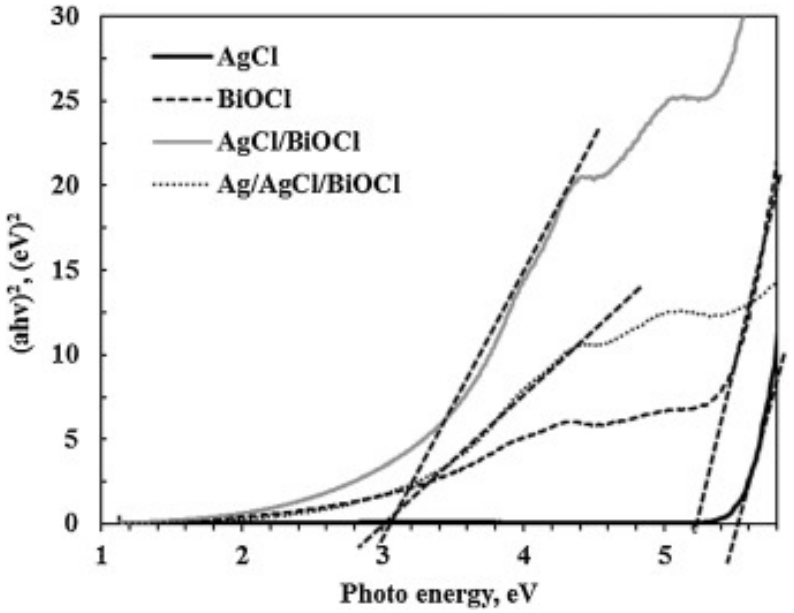

Fig. 7. Estimated optical band gap of as-synthesized particles.

3.1.6. Photodegradation under UV light irradiation

The photocatalytic degradation of phenol was carried out under UV irradiation using the ternary photocatalyst, Ag/AgCl/BiOCl. The initial catalyst loading was 0.25 g/300 mL and the effect of the UV light and the catalyst material was investigated and shown in Fig. 8. The results show a 20 % reduction in phenol concentration under adsorption conditions where the phenol solution was contacted with Ag/AgCl/BiOCl in the absence of light. The other control experiment determined the effect of the light source in the absence of the catalyst. This photolysis experiment assumes that photolytic cleavage of phenol bonds occurs under UV irradiation. Approximately 30 % degradation occurred after 4 h, therefore confirming that UV light alone is capable of partially breaking down phenol. The commonly used Degussa TiO_2 was also used under the same conditions for comparative purposes and was determined to pose similar photocatalytic activity to Ag/AgCl/BiOCl (60 %). This showed that the Ag/AgCl/BiOCl was activated in ultraviolet light and is capable of degrading phenol. The results also confirm that, for substantial degradation of phenol under UV light irradiation to occur, both light irradiation and photocatalyst are required.

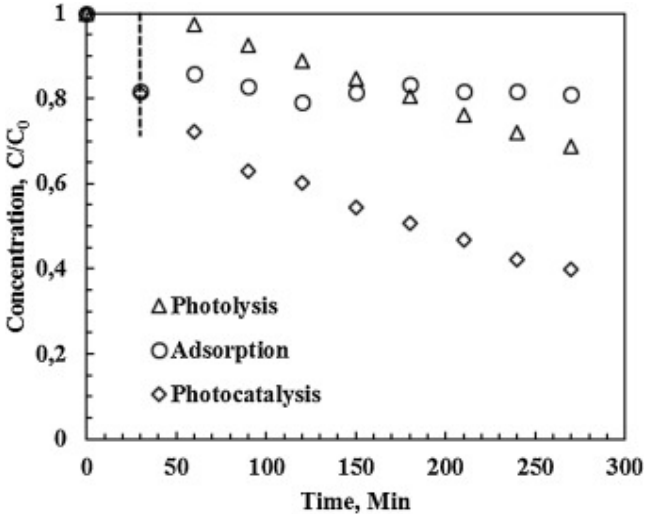

Fig. 8. Phenol degradation under UV light irradiation investigating the effect of light and photocatalyst.

The effects of the individual constituents of the photocatalysts was investigated under the same initial phenol concentration of 10 ppm under UV light irradiation (Fig. 9). The degradation efficiencies of AgCl, BiOCl, AgCl/BiOCl and Ag/AgCl/BiOCl were found to be 75 %, 47 %, 45 % and 60 % in 4 h, respectively. These results show that all synthesized catalysts are activated under UV light irradiation. AgCl showed the highest degradation activity in comparison to the other as-synthesized catalysts due to its SPR effects. AgCl is known to be a photosensitive semiconductor, therefore, it has a natural light response in the UV light region [43]. It was also noticed that the formation of metallic Ag on the AgCl/BiOCl improved its photocatalytic degradation efficiency under UV irradiation in comparison to just AgCl/BiOCl and BiOCl.

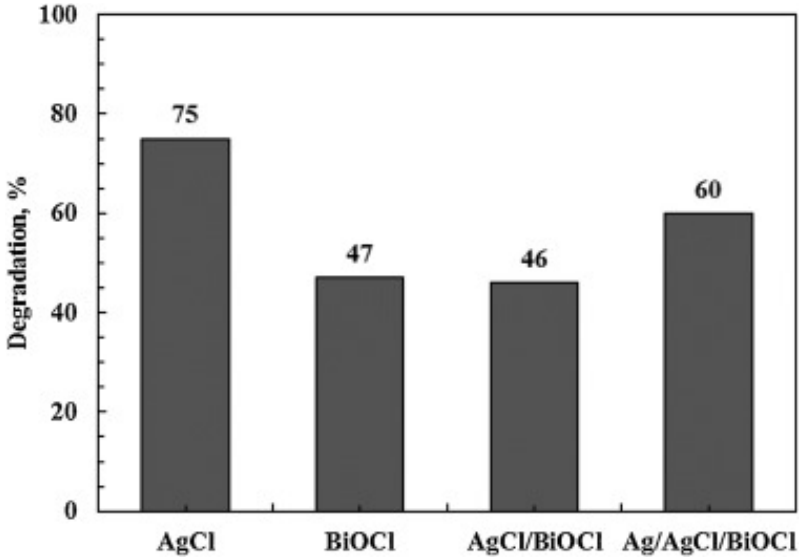

Fig. 9. AgCl, BiOCl, AgCl/BiOCl and Ag/AgCl/BiOCl under UV light irradiation.

3.1.7. Photodegradation under visible light irradiation

Under the simulated visible light, the individual effects of the light and synthesized ternary Ag/AgCl/BiOCl was investigated in the photodegradation of phenol and illustrated in Fig. 10. The photolytic degradation of phenol as a result of bond cleavage noticed under UV light irradiation was absent under visible light irradiation. While the catalyst showed 20 % degradation due to adsorption on the surface of the catalyst, the photocatalysis experiment showed 52 % phenol degradation under visible light irradiation. These results indicate that the composite catalyst is indeed activated by visible light and is capable of degrading phenol. The results presented in Fig. 10 also prove that the interaction of light and the catalyst is necessary for organic degradation to occur.

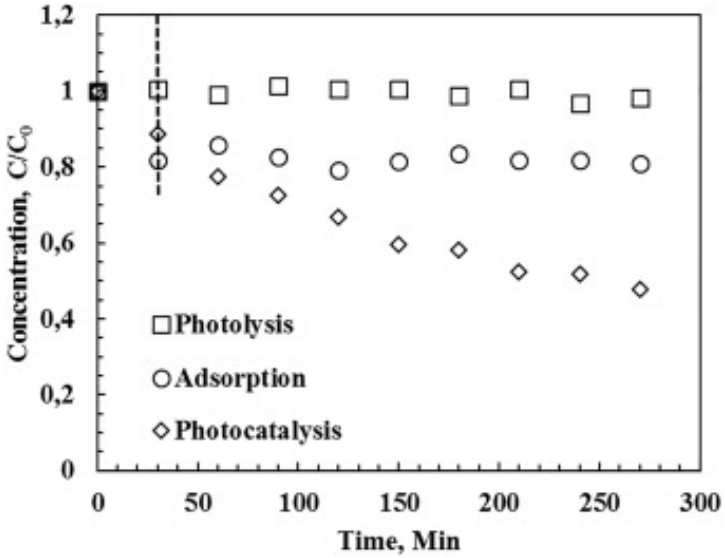

Fig. 10. Phenol degradation under visible light irradiation investigating the effect of light and photocatalyst.

Under simulated visible light irradiation, the contributions of the individual catalysts constituents was investigated and shown in Fig. 11. 14 % and 15 % reduction in phenol concentration was measured when using AgCl and BiOCl catalysts. The reduction was attributed to adsorption of phenol on the surface of the catalyst. This shows that the synthesized AgCl and BiOCl is unable to be activated by visible light in the degradation of phenol. AgCl/BiOCl and Ag/AgCl/BiOCl showed a similar degradation efficiency of 51 % and 52 % in the degradation of phenol under visible light irradiation. During the synthesis process, Ag^0 was photoreduced on the surface of AgCl/BiOCl using visible light irradiation for an hour. Therefore, Ag^0 was unavoidably generated during the phenol photocatalytic degradation reaction using AgCl/BiOCl as there was light irradiation. This means that both the binary and ternary catalyst had similar component and hence mechanism in the photodegradation of phenol.

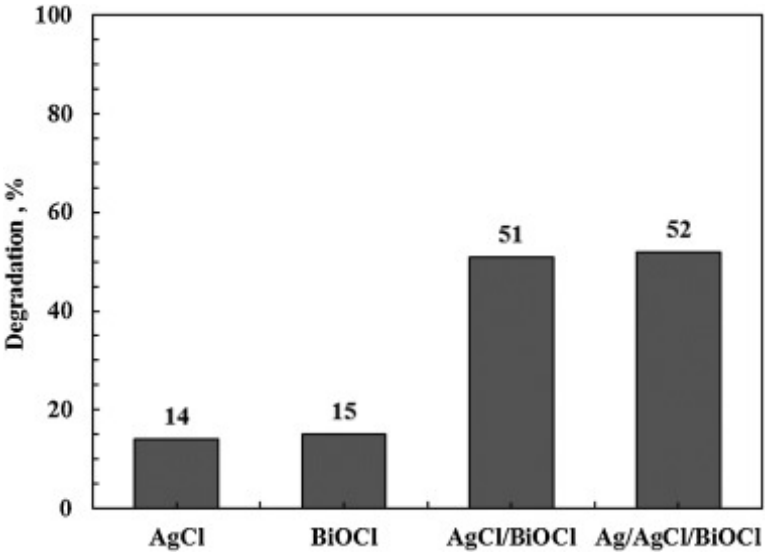

Fig. 11. AgCl, BiOCl, AgCl/BiOCl and Ag/AgCl/BiOCl under visible light irradiation.

3.2. Possible proposed mechanism

For photocatalysis to be successful, the photon energy should be greater than the bandgap of the photocatalysts [46]. Based on the phenol photocatalytic degradation experiments carried out, it was observed that AgCl and BiOCl on their own were not activated under visible light irradiation and could not generate the free radicals necessary to initiate the phenol degradation process. This was attributed to the large bandgaps determined for these materials. However, when AgCl and BiOCl were combined, and Ag^0 was photoreduced onto the surface of the AgCl, it was postulated that a heterojunction photocatalyst similar to PS—C—PS systems suggested by Zhou et al. [47] and Ye et al. [47] was formed. In this scenario, the Ag nanoparticles serve as both an electron mediator and a photosensitizer. This configuration would therefore allow for the generation of stable electron-hole pairs using low energy photons.

Charge transfer in the envisaged mechanism is theorised to occur as depicted in Fig. 12. Electron-hole pairs are initially generated in the Ag nanoparticles as a result of the surface plasmon resonance (SPR) induced by visible light illumination [42]. The electrons are then transferred to the conduction band (CB) of the AgCl, where they are further transferred to the

CB of the BiOCl. This ensures spatial separation consequently inhibiting the recombination of charges [45]. Typically the trapped electrons would then react with dissolved oxygen to form reactive superoxide free radicals ($\cdot O_2^-$). However, for this catalyst combination, it is not the case since the potential of the BiOCl CB does not favour their formation [47]. Addition of p-benzoquinone, a superoxide free radical quencher and isopropyl alcohol, a hydroxyl free radical ($\cdot OH$) quencher showed no reduction in degradation activity, this confirmed their absence in the system [47]. Further radical trapping tests carried out by the same authors while investigating the degradation of RhB dye under visible light revealed that addition of triethanolamine (TEOA) drastically reduced decolourization of the dye. This indicated that the mechanism was primarily driven by the photogenerated holes. The surface of AgCl is likely to produce free Cl^- ions, these would then react with holes on the Ag^0 surface resulting in the formation of $Cl\cdot$ free radicals. The chlorine ion on the surface of BiOCl is also reported to oxidize which adds to chlorine radical formation [48,49]. These $Cl\cdot$ free radicals would then initiate bond cleavage in the target pollutant. It should also be noted that the electrons in the CB of the BiOCl can potentially reduce the $Cl\cdot$ to Cl^-. It is postulated that a similar mechanism occurs in the present study.

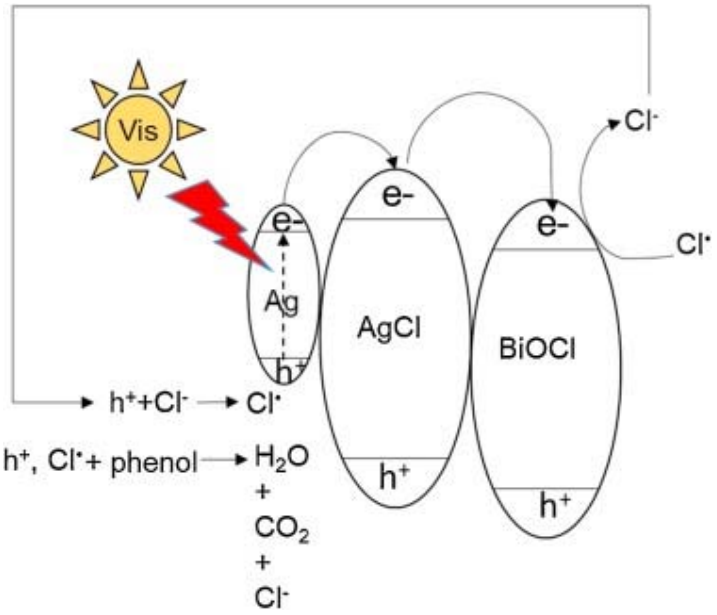

Fig. 12. Possible photocatalytic mechanism of Ag/AgCl/BiOCl in visible light degradation of phenol.

4. Conclusion

This work succeeded in the synthesis of a visible light photocatalyst Ag/AgCl/BiOCl and its constituents AgCl, BiOCl and AgCl/BiOCl. The effectiveness of the synthesis process was validated using various characterization methods to ascertain the purity, morphology and chemical states of the synthesized catalyst. The photodegradation potential of the synthesized catalysts were investigated under both ultraviolet and visible light irradiation in the degradation of aromatic carbon, phenol. The batch experiments were designed in such a way that the individual effects of light and catalysts were investigated. The results shows that all the synthesized materials are activated under UV irradiation in the degradation of phenol and due to the stability and durability of the synthesized particles; they can be used in the place of commonly used TiO_2. Both the binary AgCl/BiOCl and the ternary Ag/AgCl/BiOCl were activated in the photodegradation of phenol under visible light. This confirms the creation of

a simple and efficient photocatalyst that utilizes visible light (43 % of solar spectrum) instead of UV light (4 % of solar spectrum). This is attributed to the unique characteristics of the fabricated phototcatalysts such as the morphology, surface area, wide photoabsorption range and low recombination rates. A possible visible light photocatalytic mechanism was also postulated using the synthesized ternary photocatalyst. The creation of a ternary material resulted in a lower bandgap material viable for visible light photoabsorption. This photocatalyst shows great potential for degradation of industrial wastewater in visible light with the advantage of reducing energy costs.

CRediT authorship contribution statement

Dorcas O. Adenuga: Methodology, Formal analysis, Investigation, Writing - original draft, Project administration. **Shepherd M. Tichapondwa:** Conceptualization, Validation, Formal analysis, Resources, Supervision. **Evans M.N. Chirwa:** Conceptualization, Validation, Resources, Supervision, Funding acquisition.

Declaration of Competing Interest

The authors declare that they have no known competing financial interests or personal relationships that could have appeared to influence the work reported in this paper.

Acknowledgements

This work is based on the research supported in part by National Research Foundation of South Africa (Grant numbers: CSUR180215313534, TTK180424324064, MND190514436254) and Sedibeng Water Chair awarded to Prof EMN Chirwa.

References

[1] A.A. Mohammed, Electrocoagulation of phenol for wastewater treatment, *Iraqi J.Chem. Petrol. Eng*. 9 (3) (2007) 37–41.
[2] M.R. Hoffmann, S.T. Martin, W. Choi, D.W. Bahnemann, Environmental applications of semiconductor photocatalysis, *Chem. Rev*. 95 (1995) 69–96.
[3] X. Li, C. Zhu, Y. Song, D. Du, Y. Lin, Solvent co-mediated synthesis of ultrathin BiOCl nanosheets with highly efficient visible-light photocatalytic activity, *RSCAdv.* 7 (2017) 10235–10241, https://doi.org/10.1039/c6ra27606g.
[4] S. Xiao, D. Wan, K. Zhang, H. Qu, J. Peng, Enhanced photoelectrocatalytic degradation of ammonia by in situ photoelectrogenerated active chlorine on TiO2nanotube electrodes, *J. Environ. Sci.* (China) 50 (2016) 103–108, https://doi.org/10.1016/j.jes.2016.04.028.
[5] Y. Chen, G. Zhu, Y. Liu,J. Gao, C. Wang, R. Zhu, P. Liu, Preparation of hollow Ag/AgCl/BiOCl microspheres with enhanced photocatalytic activity for methyl orange under LED light irradiation, *J. Mater. Sci. Mater. Electron*. 28 (2016) 2859–2866, https://doi.org/10.1007/s10854-016-5870-x.
[6] Q. Wang, J. Hui, Y. Huang, Y. Ding, Y. Cai, S. Yin, Z. Li, B. Su, The preparation of BiOCl photocatalyst and its performance of photodegradation on dyes, *Mater. Sci. Semicond. Process.*17(2014) 87–93, https://doi.org/10.1016/j.mssp.2013.08.018.
[7] A. Manassero, M.L. Satuf, O.M. Alfano, Evaluation of UV and visible light activity of TiO2 catalysts for water remediation, *Chem. Eng. J*. 225 (2013) 378–386, https://doi.org/10.1016/j.cej.2013.03.097.

[8] H. Niu, Q. Wang, H. Liang, M. Chen, C. Mao, J. Song, S. Zhang, Y. Gao, C. Chen, Visible-light active and magnetically recyclable nanocomposites for the degradation of organic dye, *Materials (Basel)* 7 (2014) 4034–4044, https://doi.org/10.3390/ma7054034.
[9] M. Chowdhury, M. Ntiribinyange, K. Nyamayaro, V. Fester, Photocatalytic activities of ultra-small β-FeOOH and TiO 2 heterojunction structure under simulated solar irradiation, *Mater. Res. Bull*. 68 (2015) 133–141, https://doi.org/10.1016/j.materresbull.2015.03.044.
[10] J. Low, J. Yu, M. Jaroniec, S. Wageh, A.A. Al-Ghamdi, Heterojunction photo-catalysts, *Adv Mater* 29 (2017), https://doi.org/10.1002/adma.201601694.
[11] P. Raizada, P. Thakur, A. Sudhaik, P. Singh, V.K. Thakur, A. Hosseini-Bandegharaei, Fabrication of dual Z-scheme photocatalyst via coupling of BiOBr/Ag/AgCl heterojunction with P and S co-doped g-C3N4 for efficient phenol degradation, *Arab. J. Chem*. 13 (2020) 4538–4552, https://doi.org/10.1016/j.arabjc.2019.10.001.
[12] X. Chen, J. Hou, H. Yang, Z.-L. Xu, Facile preparation of NPs based on Ag–Ag Cl immobilized in porous PVA sphere with high visible light photoactivity and good photostability under Cl − condition, *J. Environ. Chem. Eng*. 4 (2016) 1068–1075, https://doi.org/10.1016/j.jece.2016.01.015.
[13] Q. Zhao, Y. Xing, Z. Liu, J. Ouyang, C. Du, Synthesis and characterization of modified BiOCl and their application in adsorption of low-concentration dyes from aqueous solution, *NanoscaleRes.Lett*.13 (2018), https://doi.org/10.1186/s11671-018-2480-y.
[14] A. Kumar, P.R. Thakur, G. Sharma, M. Naushad, A. Rana, G.T. Mola, F.J. Stadler, Carbonnitride, metalnitrides, phosphides, chalcogenides, perovskites and carbides nanophotocatalysts for environmental applications, *Environ. Chem. Lett*. (2018), https://doi.org/10.1007/s10311-018-0814-8.
[15] H. Cheng, B. Huang, Y. Dai, Engineering BiOX (X = Cl, Br, I) nanostructures for highly efficient photocatalytic applications, *Nanoscale* 6 (2014) 2009–2026, https://doi.org/10.1039/c3nr05529a.
[16] L. Cai, Enhanced visible light photocatalytic activity of BiOCl by compositing with g-C3N4, *Mater. Res. Innov*. 19 (2015) 392–396, https://doi.org/10.1179/1433075x15y.0000000047.
[17] P. Mytych, Z. Stasicka, Photochemical reduction of chromium (VI) byphenol and its halogen derivatives, *Appl Catal B-Environ* 52 (2004) 167–172, https://doi.org/10.1016/j.apcatb.2004.04.006.
[18] Y. Ao, H. Tang, P. Wang, C. Wang, Deposition of Ag@AgCl onto two dimensional square-like BiOCl nanoplates for high visible-light photocatalytic activity, *Mater.Lett*. 131 (2014) 74–77, https://doi.org/10.1016/j.matlet.2014.05.083.
[19] S. Zhao, Y. Zhang, Y. Zhou, K. Qiu, C. Zhang, J. Fang, X. Sheng, Reactable polyelectrolyte-assisted preparation of flower-like Ag/AgCl/BiOCl composite with enhanced photocatalytic activity, *J. Photochem. Photobiol. A: Chem*. 350 (2018)94–102, https://doi.org/10.1016/j.jphotochem.2017.09.070.
[20] D. Wei, F. Tian, Z. Lu, H. Yang, R. Chen, Facile synthesis of Ag/AgCl/BiOCl ternary nanocomposites for photocatalytic inactivation of S. Aureus under visible light, *RSC Adv*. 6 (2016) 52264–52270, https://doi.org/10.1039/c6ra05754c.
[21] M. Zhao, W. Zhou, M. Lu, Z. Guo, C. Li, W. Wang, Novel AgCl nanotubes/BiOCl nanosheets composite with improved adsorption capacity and photocatalytic performance, *J. Alloys. Compd*. 773 (2019) 1146–1153, https://doi.org/10.1016/j.jallcom.2018.09.257.
[22] Q. Li, G. Duan, J. Luo, X. Liu, Ultrasonic-assisted synthesis of plasmonic Z-schemeAg/ AgCl/WO3-nanoflakes photocatalyst in geothermal water with enhanced visible-light photocatalytic performance, *J. Energy Chem*. 27 (2018) 826–35, https://doi.org/10.1016/j.jechem.2017.05.011.

[23] L. Xia, X. Jiang, Z. Cheng, Y. Liao, Z. Wang, Q. Pu, M. Duan, Synthesis of Pp-16@Ag/AgCl of high performance photocatalyst particles for decomposition of Rhodamine B and fast green dyes, *Mater.Chem.Phys*.218(2018)98–107, https://doi.org/10.1016/j.matchemphys.2018.07.032.
[24] Z. Feng, J. Yu, D. Sun, T. Wang, Visible-light-driven photocatalysts Ag/AgCl dispersed on mesoporous Al2O3 with enhanced photocatalytic performance, *J. ColloidI nterface Sci.* 480 (2016) 184–190, https://doi.org/10.1016/j.jcis.2016.06.068.
[25] S. Huang, J. Chen, J. Zhong, J. Li, W. Hu, M. Li, K. Huang, R. Duan, Enhanced photocatalytic performance of Ag/AgCl/SnO2 originating from efficient formation of O 2 −, *Mater. Chem. Phys*. 201 (2017) 35–41, https://doi.org/10.1016/j.matchemphys.2017.08.024.
[26] R. Adhikari, G. Gyawali, T. Sekino, S. Wohn Lee, Microwave assisted hydrothermal synthesis of Ag/AgCl/WO3 photocatalyst and its photocatalytic activity under simulated solar light, J. Solid State Chem. 197 (2013) 560–565, https://doi.org/10.1016/j.jssc.2012.08.012.
[27] X. Li, D. Wu, Q. Luo, R. Yin, J. An, S. Liu, D. Wang, Fabrication of CPAN/Ag/AgCl composites and their efficient visible-light photocatalytic activity, *J. Alloys. Compd.*702 (2017) 585–593 ,https://doi.org/10.1016/j.jallcom.2017.01.289.
[28] X.-J. Wen, C.-G. Niu, L. Zhang, D.-W. Huang, G.-M. Zeng, In-situ synthesis of visible-light-driven plasmonic Ag/AgCl-CdWO4 photocatalyst, *Ceram. Int*. 43 (2017)1922–1929, https://doi.org/10.1016/j.ceramint.2016.10.153.
[29] S. Lou, W. Wang, L. Wang, S. Zhou, In-situ oxidation synthesis of Cu2O/Ag/AgCl microcubes with enhanced visible-light photocatalytic activity, *J. Alloys. Compd*.781 (2019) 508–514, https://doi.org/10.1016/j.jallcom.2018.12.115.
[30] Y. Xu, D. Lin, X. Liu, Y. Luo, H. Xue, B. Huang, Q. Qian, Q. Chen, TiO 2 hollow nanofibers grafted Ag/AgCl with more AgCl {1 1 1} facet for enhanced photo-catalytic activity, *Mater. Lett*. 215 (2018) 250–253, https://doi.org/10.1016/j.matlet.2017.12.100.
[31] A.S. Ganeshraja, K. Zhu, K. Nomura, J. Wang, Hierarchical assembly of AgCl@Sn-TiO2 microspheres with enhanced visible light photocatalytic performance, *Appl.Surf. Sci.* 441 (2018) 678–687, https://doi.org/10.1016/j.apsusc.2018.01.262.
[32] L. Dai, R. Liu, L.Q. Hu, C.L. Si, Simple and green fabrication of AgCl/Ag-cellulose paper with antibacterial and photocatalytic activity, *Carbohydr. Polym.*174(2017)450–455, https://doi.org/10.1016/j.carbpol.2017.06.107.
[33] J.F. Guo, B. Ma, A. Yin, K. Fan, W.L. Dai, Highly stable and efficient Ag/AgCl@TiO2photocatalyst: preparation, characterization, and application in the treatment of aqueous hazardous pollutants, *J. Hazard. Mater*. 211-212 (2012) 77–82, https://doi.org/10.1016/j.jhazmat.2011.11.082.
[34] S. Hong, T. Ratpukdi, J. Sivaguru, E. Khan, Glutaraldehyde removal from produced waters USing visible light driven photocatalysis, WEFTEC (2017).
[35] D. Adenuga, S. Tichapondwa, E. Chirwa, Synthesis and Characterisation of Potential Visible-light Photocatalyst and its photocatalytic activity in the decomposition of phenol, *Chem. Eng. Trans*. 74 (2019), https://doi.org/10.3303/CET1974182.
[36] W. Xu, Y. Zhang, T. Chen, Single Particle *Nanocatalysis: Fundamentals and Applications*, Wiley-VCH, Changchun, 2019.
[37] X.F. Zhang, Z.G. Liu, W. Shen, S. Gurunathan, Silver nanoparticles: synthesis, characterization, properties, applications, and therapeutic approaches, *Int. J. Mol. Sci*. 17 (2016), https://doi.org/10.3390/ijms17091534.
[38] M.S. Al Aboody, Silver/silver chloride (Ag/AgCl) nanoparticles synthesized from Azadirachta indica lalex and its antibiofilm activity against fluconazole resistantCandida tropicalis, *Artif. Cells Nanomed. Biotechnol*. 47 (2019) 2107–2113, https://doi.org/10.1080/21691401.2019.1620257.

[39] P. Singh, P. Sonu, A. Raizada, P. Sudhaik, P. Shandilya, S. Agarwal Thakur, V.K. Gupta, Enhanced photocatalytic activity and stability of AgBr/BiOBr/graphene heterojunction for phenol degradation under visible light, *J. Saudi Chem. Soc*.(2018), https://doi.org/10.1016/j.jscs.2018.10.005.
[40] F. Dong, X. Feng, Y. Zhang, C. Gao, Z. Wu, An anion-exchange strategy for 3D hierarchical (BiO)2CO3/amorphous Bi2S3 heterostructures with increased solar absorption and enhanced visible light photocatalysis Electronic supplementary in-formation (ESI) available. See DOI:.doi:10.1039/c4ra15798b,RSCAdv.5(2015)11714–11723.
[41] D. Sun, J. Li, Z. Feng, L. He, B. Zhao, T. Wang, R. Li, S. Yin, T. Sato, Solvothermal synthesis of BiOCl flower-like hierarchical structures with high photocatalytic activity, *Catal. Commun*. 51 (2014) 1–4, https://doi.org/10.1016/j.catcom.2014.03.004.
[42] W. Cui, X. Li, C. Gao, F. Dong, X. Chen, Ternary Ag/AgCl-(BiO)2 CO3 composites as high-performance visible-light plasmonic photocatalysts, *Catal. Today* 284(2017) 67–76, https://doi.org/10.1016/j.cattod.2016.10.020.
[43] H. Daupor, S. Wongnawa, Urchinlike Ag/AgCl photocatalyst: synthesis, characterization, and activity, *Appl. Catal. A Gen*. 473 (2014) 59–69, https://doi.org/10.1016/j.apcata.2013.12.036.
[44] C.-C. Chen, C.-T. Yang, W.-H. Chung, J.-L. Chang, W.-Y. Lin, Synthesis and characterization of Bi4Si3O12, Bi2SiO5, and Bi12SiO20 by controlled hydrothermal method and their photocatalytic activity, *J. Taiwan Inst. Chem. Eng.* 78 (2017)157–167, https://doi.org/10.1016/j.jtice.2017.05.021.
[45] L. Ye, J. Liu, C. Gong, L. Tian, T. Peng, L. Zan, Two different roles of metallic AgonAg/AgX/BiOX(X =Cl, Br) visible light photocatalysts: surface plasmon resonance and Z-Scheme bridge, *ACS Catal.* 2 (2012) 1677–1683, https://doi.org/10.1021/cs300213m.
[46] S. Zhu, D. Wang, Photocatalysis:basic principles, diverse forms of implementations and emerging scientific opportunities, *Adv. Energy Mater*. 7 (2017), https://doi.org/10.1002/aenm.201700841.
[47] P. Zhou, J. Yu, M. Jaroniec, All-solid-state Z-scheme photocatalytic systems, *Adv Mater* 26 (2014) 4920–4935, https://doi.org/10.1002/adma.201400288.
[48] W. Xiong, Q. Zhao, X. Li, D. Zhang, One-step synthesis of flower-like Ag/AgCl/BiOCl composite with enhanced visible-light photocatalytic activity, *Catal. Commun*. 16 (2011) 229–233, https://doi.org/10.1016/j.catcom.2011.09.027.
[49] W. Zhang, Xa. Dong, Y. Liang, Y. Sun, F. Dong, Ag/AgCl nanoparticles assembled on BiOCl/Bi12O17Cl2 nanosheets: enhanced plasmonic visible light photocatalysis and in situ DRIFTS investigation, *Appl. Surf. Sci*.455(2018)236–243, https://doi.org/10.1016/j.apsusc.2018.05.171.